Journal of Quantitative Spectroscopy & Radiative Transfer 113 (2012) 878–888

Contents lists available at SciVerse ScienceDirect

Journal of Quantitative Spectroscopy & Radiative Transfer

journal homepage: www.elsevier.com/locate/jqsrt

High resolution Fourier transform spectroscopy of $HD^{16}O$: Line positions, absolute intensities and self broadening coefficients in the 8800–11,600 cm^{-1} spectral region

Ludovic Daumont [a,*], Alain Jenouvrier [a], Semen Mikhailenko [b], Michel Carleer [c], Christian Hermans [d], Sophie Fally [d], Ann Carine Vandaele [d]

[a] Groupe de Spectrométrie Moléculaire et Atmosphérique, UMR CNRS 6089, UFR Sciences, Moulin de la Housse, B.P. 1039, 51067 Reims Cedex 2, France
[b] Laboratory of Theoretical Spectroscopy, V.E. Zuev Institute of Atmospheric Optics, SB RAS, 1, Akademician Zuev square, 634021 Tomsk, Russia
[c] Service de Chimie Quantique et de Photophysique, CP 160/09, Université Libre de Bruxelles, 50 Av. F. D. Roosevelt, B-1050 Brussels, Belgium
[d] Institut d'Aéronomie Spatiale de Belgique, Av. Circulaire 3, B-1180 Brussels, Belgium

ARTICLE INFO

Available online 18 February 2012

Keywords:
Water vapor
H_2O
Line intensity
Broadening
Atmospheric absorption
Fourier transform spectroscopy
$HD^{16}O$
Deuterium

ABSTRACT

High-resolution water vapor absorption spectra have been measured at room temperature in the 8800–11,600 cm^{-1} spectral region. They were obtained using the mobile BRUKER IFS 120M Fourier transform spectrometer (FTS) from ULB-SCQP coupled to the 50 m base long multiple reflection White type cell in GSMA laboratory. The absorption path was 600 m and different $H_2O/HDO/D_2O$ mixtures were used. Measurements of line positions, intensities and self-broadening coefficients were performed for the $HD^{16}O$ isotopologue. 6464 rovibrational assignment of the observed lines was made on the basis of global variational predictions and allowed the identification of new energy levels. $3\nu_3$, $2\nu_1+\nu_3$, $3\nu_1+\nu_2$, $\nu_1+2\nu_3$ and $2\nu_2+2\nu_3$ are the five strongest bands. The present paper provides a complementary data set on water vapor for atmospheric and astrophysical applications.

1. Introduction

Significant developments of remote sensing techniques have occurred recently and will continue to occur in the near future. In particular, satellite instruments such as *AIRS* (Atmospheric Infrared Sounder) on Aqua [1], *ACE-FTS* Atmospheric Chemistry Experiment on SCISAT [2], *MLS* (Microwave Limb Sounder) [3], *TES* (Tropospheric Emission Spectrometer) on the Aura platform [4], *IASI* (Infrared Atmospheric Sounding Interferometer) on MetOP-A [5] and *MIPAS* (Michelson Interferometer for Passive Atmospheric Sounding) on ENVISAT [6] have higher detection limits or better detection capabilities for minor species of small abundances than previous missions. These enhancements call for parallel improvements of basic spectroscopic parameters. The specific spectroscopic needs concern overall more accurate parameters but also new or more extended spectroscopic data, e.g. new species, weak lines, additional molecular bands.

The interest of the mono-deuterated water molecule (HDO) is not only atmospheric but is also of great importance for astrophysics observations. It can be used to characterize brown dwarfs, very low mass stars and planets [7–10]. It can help to understand climatic evolution of planets and has been detected in many interstellar media [11].

This isotopologue has also some theoretical interest because the substitution of one hydrogen atom by a deuterium atom gives rise to very different harmonic frequencies from those of H_2O, which greatly changes

* Corresponding author. Tel./fax: +33 3 26 91 33 33.
E-mail address: ludovic.daumont@univ-reims.fr (L. Daumont).

0022-4073/$ - see front matter © 2012 Elsevier Ltd. All rights reserved.
doi:10.1016/j.jqsrt.2012.02.017

the intra-molecular dynamics [12,13]. Changes of symmetry from H_2O to HDO gives important information on the bifurcation schemes for the different isotopologues and then allow to understand how to assign the high energy rovibrational levels with physical consistency [14].

Continuing our previous works concerning the water vapor molecule in the frame of a long-term French–Belgian collaboration [15–17] (and references therein), the present paper investigates the $HD^{16}O$ isotopologue in the 8800–11,600 cm^{-1} spectral range. It complements and extends two of our earlier studies about $HD^{16}O$ covering the 11,500–23,000 cm^{-1} region [12,18]. The huge amount of information contained in the spectra leads us to proceed in the following way. First the isotopologue type ($H_2^xO/HD^xO/D_2^xO$) is experimentally identified for each line as described in Section 3. Then the rovibrational assignment – based on difference combinations – allowed identifying the complete species (^{16}O, ^{18}O). The absorption line parameters were then determined using the corresponding isotopologue mass for the Doppler line width parameter. As a result, the spectral information for the isotopologues $HD^{18}O$ and $D_2^{18}O$ covering the same spectral region was published separately in [13,19]. Although ^{18}O is present in natural abundance in the samples, the lines of these two species are detected in the spectra. All our previous measurements on $H_2^{18}O$, $H_2^{17}O$, $HD^{16}O$ and $HD^{18}O$ species have been analysed through the IUPAC (International Union of Pure and Applied Chemistry) critical evaluation of the rotational-vibrational spectra of water vapor [20,21].

The $HD^{16}O$ spectrum in this region has been the subject of several studies [22–30] based on four experimental techniques: ICLAS (IntraCavity LAser Spectrometer), ICLAS-VECSEL (Vertical External Cavity Surface Emitting Laser), PAS (PhotoAcoustic Spectroscopy) and FTS (Fourier Transform Spectrometer). Most of these concentrate on the determination of lines positions and on the rovibrational analysis; they provide assignments and upper energy levels with accuracy close to the experimental uncertainty. Five of them [23,25–28] give rotational, centrifugal distortion, vibrational and coupling constants using the effective Hamiltonian approach. In these papers, the stated accuracies for the line positions are limited to 0.001 cm^{-1} in the best case for resolutions ranging between 0.04 and 0.005 cm^{-1}. Bykov et al. [23] mentioned that they analysed relative line strengths but these authors do not report these values. Bertseva et al. [27] and Naumenko et al. [28] have performed rough intensities estimates for identification purposes but do not report them either. Only Ulenikov et al. [29] have determined absolute line intensities but they had to make the assumption that the 1:1 mixture of the D_2O and H_2O samples leads to 50% of HDO. To our knowledge, there are no studies reporting line broadening parameters. Although a major addition has been made in the most recent version of the HITRAN database [31] with 3528 $HD^{16}O$ transitions in the 11600 to 23,000 cm^{-1} spectral region, the database only contains 127 $HD^{16}O$ transitions in the 8800–11,600 cm^{-1} wavenumber range. Twelve of them belong to the $2\nu_2+2\nu_3$, five to the $\nu_1+2\nu_3$ band and one hundred and ten to the $3\nu_3$ band.

The present paper is devoted to the accurate determination of $HD^{16}O$ line positions, absolute line intensities and rovibrational assignments in the 8800–11,600 cm^{-1} range, the partial pressures of the isotopologue being determined only through spectroscopic measurements.

After a brief description of the experimental set-up and more detailed explanations about the procedure of data analysis in Sections 2 and 3, the determination of partial pressures will be explained in Section 4. The rovibrational assignments are discussed in Section 5. The results including all the line parameters will be discussed with regard to the most recent experimental data and calculations in Section 7.

2. Experimental conditions

As was already done in the upper region from 13,000 to 26,000 cm^{-1} [32] the $D_2O/HDO/H_2O$ mixture's spectra were recorded with the experimental set-up made up of the 50 m base long absorption cell [33] in the configuration that correspond to an absorption path length of 602 m. Spectra were recorded at high-resolution with a Bruker IFS 120M FTS (thereafter called ULB/IASB FTS). The unapodized resolution (0.03 cm^{-1}, which corresponds to 30 cm of MOPD with the Bruker definition) is lower than or close to the full width of the lines in our experimental conditions.

The cell was set with $Al+MgF_2$ coated mirrors and CaF_2 windows. A 450W Xenon lamp (Hanovia 976) was used as light source in combination with different optical filters. A Si diode detector sensitive over the whole spectral range investigated was used. The co-addition of 1024 interferograms, leading to a total recording time of 19 h, proved to be adequate to obtain a root mean square (RMS) signal-to-noise (S/N) ratio (expressed as the maximum signal amplitude divided by twice the RMS noise amplitude) ranging from 2100 up to 3600. All the spectra were recorded at room temperature (292 K $\pm$ 2 K), which was monitored in the cell by three platinum resistance thermometers placed on the walls of the cell at its center and its two ends. The temperature along the cell was not stabilized, so that differences between the two ends of the cell, of the order of 2 K, were sometimes observed. The atmospheric water absorption occurring along the path between the cell and the spectrometer was not taken into account because the HDO lines are negligible in that short path at natural abundance. The pressure was measured with a MKS Baratron capacitance manometer. The water vapor samples were carefully degassed in the liquid phase. The natural sample was prepared from tri-distilled liquid water. The sample of $D_2^{16}O$, purchased from the Commissariat à l'Energie Atomique (CEA), was not pure and an estimation from the partial pressures determined in the spectra gives only 74.2% of D_2O. The oxygen was assumed to be at natural abundance in each sample. In order to avoid condensation on the inner mirrors and on the cell windows and walls, the partial pressures were selected to be well below the saturated vapor pressure. For both pure and mixed samples, measurements were performed after a period of several hours after the filling of the cell allowing for pressure and temperature stabilization as well as dilution homogenisation.

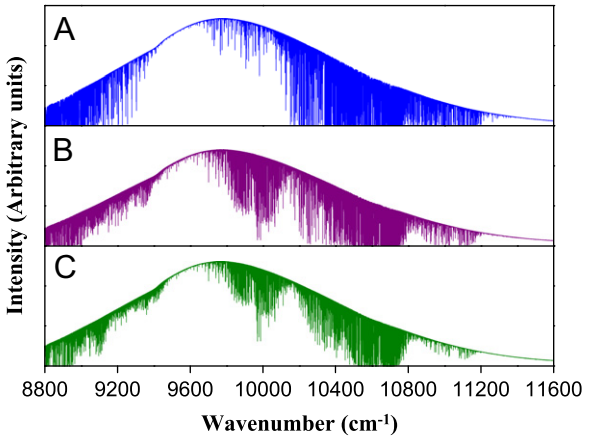

Fig. 1. The 8800–11600 cm^{-1} spectral range absorption spectra. (A) Natural water, (B) 50%–50% mixture of the natural water and D_2O samples and (C) D_2O sample.

ULB/IASB FTS was operated in air and the wavenumber scale were calibrated using our previous work on natural abundance H_2O spectra [15] for lines in the region 9350–10,500 cm^{-1} and from HITRAN 2008 [31] for some lines in the region 9000–9100 cm^{-1}. A fitted calibrating curve $\nu(\mathrm{ref})_{\mathrm{vacuum}}-\nu(\mathrm{obs})_{\mathrm{air}}=2.0339\times10^{-2}+2.15\times10^{-6}\nu(\mathrm{obs})_{\mathrm{air}}$ was applied to convert the observed line positions in air into calibrated vacuum wavenumbers. This calibration carried over 236 lines of $H_2^{16}O$ results in a 0.003 cm^{-1} root mean square accuracy, which is of the order of the expected accuracy. It must be noted that the measured line positions are determined in water spectra at pressures around 10 hPa (except for the strongest lines) meaning that pressure-induced shifts were not taken into account. An estimate of the shifts leads to maximum displacements that are less than 10^{-3} cm^{-1} with positive and negative values leading to an average that is far lower. Fig. 1 plots the three spectra recorded and shows the amount of lines that had to be treated.

3. Isotopologues identification

In the measurement and assignment processes, the first step was to identify the isotopologue responsible for each absorption line. This identification is needed, first to measure the line parameters using the real Doppler line width in the profile, and then to prepare a clean line list for the ro-vibrational assignment. The identification was obtained using the direct ratio of the spectra as shown in Fig. 2. Three spectra with approximately the same total pressure (around 10 hPa) was used, one in natural concentration: A, one with the D_2O sample: C and one with a 50%–50% volume mixture of the latter two: B. Due to H and D exchange between the water species, the mixing ratios of each isotopologue is different in each spectra. As no difference has ever been noticed between the pressure broadenings due to different isotopologues, the line shapes are approximately the same in each spectrum. Hence in the spectra ratio, the species that decrease their concentrations and the one that increase their concentrations appear upward and downward, respectively. The first step has then consisted in preparing a first line list with the approximate positions of all the lines. In the second step, we used the spectra ratio B/A and noticed that the upward lines belonged to H_2O whereas the downward ones belonged either to HDO or D_2O. Then the second spectra ratio C/B were used to notice that the downward lines belonged to D_2O whereas the upward ones belonged either to HDO or H_2O.

At that step we had a line list of approximate line positions with the assignment to each isotopologue. This list was used to begin the determination of the parameters for each line.

4. Partial pressure determination

Once the isotopologue was known, we used the Wspectra [34] and Bfit [35] softwares developed in ULB to adjust each line to a Voigt profile and determine the line positions, surfaces (integrated absorption coefficients) and Lorentzian widths. We then determined for each isotopologue the mean ratios of the line surface between two spectra, which is the ratio of the partial pressures.

We thus have the measured total pressures

$$\begin{cases} P_A = P_A^{H_2O} + P_A^{HDO} + P_A^{D_2O} \\ P_B = P_B^{H_2O} + P_B^{HDO} + P_B^{D_2O} \\ P_C = P_C^{H_2O} + P_C^{HDO} + P_C^{D_2O} \end{cases}$$

In the natural abundance spectrum A, the partial pressures are known. For the H_2O isotopologue in spectra B and C the absolute intensities reported in our previous work [15] and in HITRAN 2008 [31] were used to determine the partial pressures $P_B^{H_2O}$ and $P_C^{H_2O}$. The two remaining constraints are thus given by the mean surface ratios: $\alpha=(P_B^{HDO}/P_C^{HDO})=2.18(14)$ and $\beta=(P_B^{D_2O}/P_C^{D_2O})=0.450(34)$. The precision on the resulting partial pressures is also determined by the precision of the pressure measurements and of the surface ratio determinations. It gives the following mixing ratios: in spectra C: H_2O:3.1%/HDO:22.7%/D_2O:74.2% and in spectra B: H_2O:16.5%/HDO:49.9%/D_2O:33.6%.

One can notice that the method of surface ratio has already been used for instance in [36] but with the additional assumption that the exchange reaction of H and D between water molecules follows the statistical distribution and that the initial mole quantity of H_2O and D_2O is the same. Subsequent works on the fundamental bands such as [37] could only rely on this assumption.

5. Assignments of the $HD^{16}O$ lines in the 8800–11,600 cm^{-1}

A set of 6465 transitions of the $HD^{16}O$ molecule has been assigned in the 8800–11,600 cm^{-1} region. Table 1 gives the spectral regions, the number of transitions and the maximal values of the rotational numbers J and K_a for the 29 bands. Results of previous studies of the $HD^{16}O$ absorption spectra in this region have been published in [15,16,22–30]. According to the recent review of the IUPAC task group [21], overall 5291 transitions have been observed in these previous studies between 8800

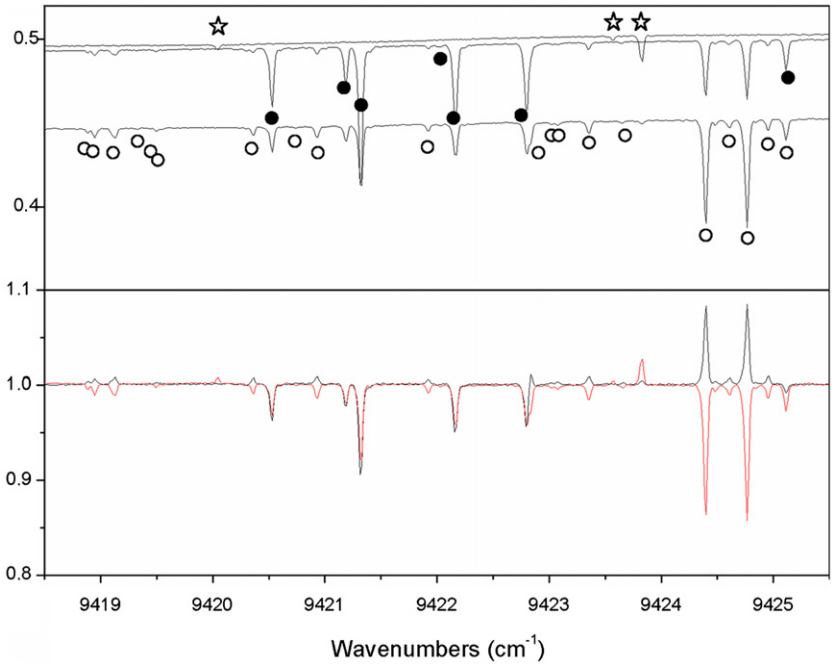

Fig. 2. Sample of spectra with isotopologue assignment from the spectra ratio around 9420 cm^{-1}. The HDO rovibrational line assignments are given in Table 2 as example. The H_2O lines are marked with stars, HDO ones with empty circles and D_2O ones with full circles. The upper panel show the spectra A, B and C, the lower panel show the two spectra ratio: C/B and B/A.

Table 1
Statistics of the observed transitions of the $HD^{16}O$ molecule.

Band	Range (cm^{-1})		Number of assignments	J, K_a max		Observed intensities at (292 K)		
						Minimum	Maximum	Sum
v_2+2v_3	8800	9133	176	16	8	2×10^{-26}	2×10^{-23}	1.45×10^{-22}
$2v_1+v_3$	8801	9510	549	14	8	3×10^{-27}	6×10^{-24}	3.41×10^{-22}
$v_1+2v_2+v_3$	8841	9620	337	13	7	2×10^{-27}	2×10^{-24}	9.46×10^{-23}
$4v_2+v_3$	8917	9634	297	13	7	2×10^{-27}	2×10^{-24}	3.48×10^{-23}
$3v_2+v_3$	8964	8964	1	9	1	2×10^{-26}	2×10^{-26}	2.29×10^{-26}
$7v_2$	8979	9662	200	11	3	3×10^{-27}	8×10^{-25}	2.20×10^{-23}
$3v_1+v_2$	9012	9728	740	15	8	2×10^{-27}	4×10^{-24}	1.96×10^{-22}
v_1+5v_2	9074	9804	216	13	4	1×10^{-27}	2×10^{-25}	6.52×10^{-24}
$v_1+3v_2+v_3-v_2$	9145	9145	1	4	0	9×10^{-27}	9×10^{-27}	9.10×10^{-27}
$2v_1+3v_2$	9146	9817	316	13	5	2×10^{-27}	2×10^{-25}	8.37×10^{-24}
$3v_1+2v_2-v_2$	9193	9193	1	3	2			
$3v_3-v_2$	9197	9282	4	3	2	7×10^{-27}	8×10^{-27}	1.44×10^{-26}
$8v_2$	9266	10,704	14	12	3	2×10^{-26}	1×10^{-25}	8.84×10^{-25}
$6v_2$	9283	9300	2	7	2	1×10^{-25}	1×10^{-25}	1.40×10^{-25}
v_1+2v_3	9470	10,194	907	17	8	1×10^{-27}	1×10^{-23}	5.92×10^{-22}
$2v_2+2v_3$	9534	10,729	777	17	9	2×10^{-27}	1×10^{-23}	6.42×10^{-22}
$3v_2+2v_3-v_2$	9666	10,036	67	11	5	2×10^{-27}	6×10^{-26}	7.18×10^{-25}
$v_1+v_2+2v_3-v_2$	9733	9963	11	7	3	2×10^{-27}	2×10^{-26}	4.86×10^{-26}
$4v_1$	10,074	10,637	304	13	7	1×10^{-26}	3×10^{-24}	1.50×10^{-22}
$3v_3$	10,086	11,038	1166	18	9	7×10^{-27}	1×10^{-22}	1.01×10^{-20}
$5v_2+v_3$	10,107	10,713	43	14	3	4×10^{-27}	2×10^{-24}	8.59×10^{-24}
$2v_1+v_2+v_3$	10,257	10,694	70	9	5	9×10^{-27}	5×10^{-25}	8.86×10^{-24}
$v_1+3v_2+v_3$	10,368	10,719	22	9	3	1×10^{-26}	1×10^{-24}	4.96×10^{-24}
$v_2+3v_3-v_2$	10,457	10,655	28	6	5	2×10^{-26}	3×10^{-25}	1.63×10^{-24}
$3v_1+2v_2$	10,471	10,740	27	9	3	4×10^{-26}	2×10^{-23}	3.45×10^{-23}
$2v_1+4v_2$	10,829	10,829	2	3	3	6×10^{-27}	6×10^{-27}	6.41×10^{-27}
$3v_2+2v_3$	11,105	11,489	67	9	6	2×10^{-26}	5×10^{-25}	3.70×10^{-24}
$v_1+v_2+2v_3$	11,186	11,491	95	9	4	3×10^{-26}	5×10^{-25}	1.48×10^{-23}
$3v_1+v_3$	11,432	11,599	24	7	3	2×10^{-26}	1×10^{-25}	1.83×10^{-24}
Total	8800	11,600	6464	18	9	1×10^{-27}	1×10^{-22}	1.24×10^{-20}

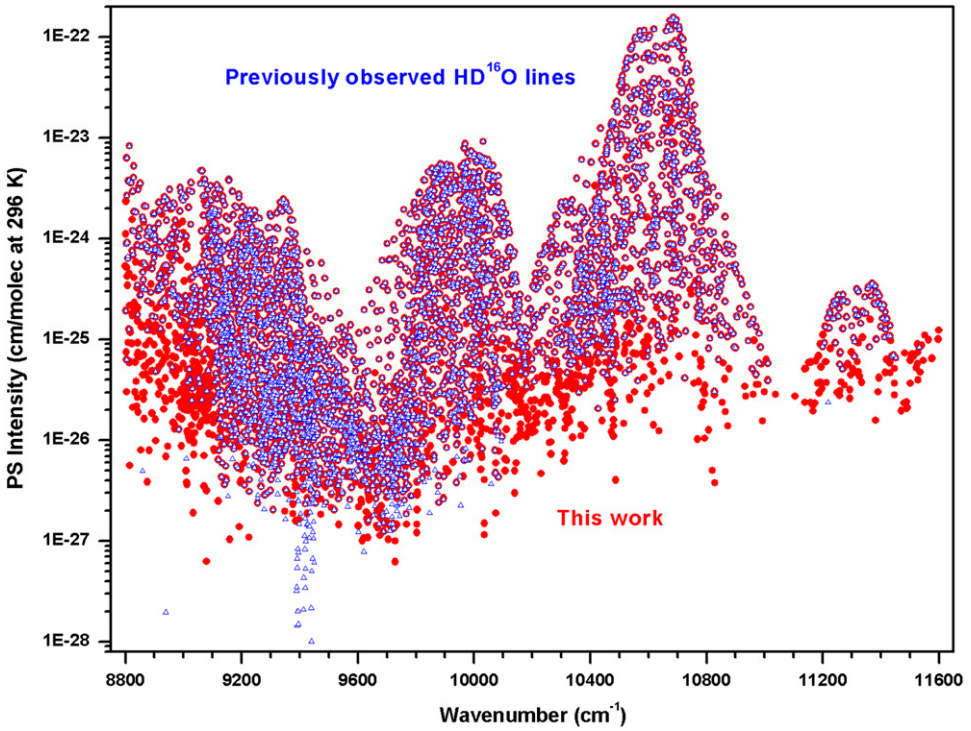

Fig. 3. Spectrum of $HD^{16}O$ containing all assigned lines in the region 8800–11,600 cm^{-1}. Triangles represent lines assigned in previous works (only line positions was then observed).

and 11600 cm^{-1}. As it is mentioned in the introduction, only 127 transitions of three bands ($3\nu_3$, $\nu_1+2\nu_2$ and $2\nu_2+2\nu_3$) are included in the current version of HITRAN database [31]. Fig. 3 shows the lines assigned in this work with the lines already assigned in previous works marked as triangles. The intensities plotted are those from PS calculation since in most previous work no information is provided about absolute intensities.

Lines assignments have been made using the results of [27,28,30] (so called "trivial assignment") and on the theoretical calculation of the vibration-rotation spectrum of $HD^{16}O$, which was made by S.A. Tashkun. This list is available at http://spectra.iao.ru. Calculation is based on the PES [38] and DMS [39] given by Partridge and Schwenke. Hereafter, we shall refer to these calculations as PS line list. Note that the vibrational labeling of assigned lines is not always clear for this spectral region. As a result, the vibrational labeling of the same lines can be different, for example, in Ref. [29] and Ref. [30]. We used the labeling of Refs. [27,28] in case of "trivial assignment". As a rule, we used the labeling of the PS calculation for the assignments of the lines observed for the first time. Both known experimental energy levels and PS line list allow us to assign about 6500 transitions of 29 bands of $HD^{16}O$ (see Table 1). On the final step the RITZ code [13] was used to check the consistency of the vibration-rotation transitions assignments and to determine the energies for the upper levels.

General comparison of observed (ν^{OBS}) and calculated (ν^{PS}) line positions is shown in Fig. 4. This plot demonstrates the good quality of the theoretical predictions of all bands between 8800 and 11,600 cm^{-1}. Most of the $\Delta\nu=(\nu^{OBS}-\nu^{PS})$ differences are within 0.3 cm^{-1}. This is quite enough to assign with confidence practically all lines. The biggest discrepancies between observed and calculated line positions are for the $4\nu_1$ and $3\nu_1+\nu_2$ bands (Fig. 5). Maximal values of the $\Delta\nu$ differences are for the lines shown in (Fig. 5) that is

- the $3\nu_3$ band, $\Delta\nu=-0.41$ cm^{-1}, upper level of the (003) state, $J=7$, $K_a=1$, $K_c=6$;
- the $3\nu_1+2\nu_2$ band, $\Delta\nu=+0.45$ cm^{-1}, upper level of the (320) state, $J=7$, $K_a=1$, $K_c=6$;
- the $8\nu_2$ band, $\Delta\nu=-1.15$ cm^{-1}, upper level of the (080) state, $J=6$, $K_a=0$, $K_c=6$.

These big discrepancies are due to strong vibration-rotation Coriolis and Fermi interactions between rotational levels of different vibrational states. According to [28] a part of the rotational levels of the (003) state is strongly perturbed by the interactions with the (320), (131), (051) and (080) states. It explains big differences for the $3\nu_3$, $3\nu_1+2\nu_2$ and $8\nu_2$ bands. The same, levels of the (400) state are mixed with those of the (131), (051) and (150) states [28]. The lines of the $3\nu_1+\nu_2$ band (upper state (310)) are in resonance with lines of the $2\nu_1+\nu_3$ and $\nu_1+2\nu_2+\nu_3$ bands (upper states (201) and (121)) [29].

Assigned transitions allow us to determine 289 new and four corrected rotational levels of 21 vibrational states. The corresponding 293 energy levels are listed in Table 3. The values of four levels are enough different

Table 2
Sample assignment of the HDO lines shown in Fig. 2. Two lines have a double assignment. One is blended with a D_2O line.

Mol	Assignments								E_{low} (cm^{-1})	Nu_obs (cm^{-1})	*d*Nu (cm^{-1})	I_obs, (cm/molec) (292 K)	*dI*, (cm/molec) (292 K)	Gself (cm^{-1}/atm)	*dG* (cm^{-1}/atm)	Comment
	V'	J'	K_a'	K_c'	V''	J''	K_a''	K_c''								
14	310	9	5	5	000	9	4	6	949.5772	9418.9252	0.0012	2.552E−26	2.2E−28	0.4978	0.0422	
14	230	4	1	3	000	5	1	4	265.2360	9418.9894	0.0004	5.809E−26	1.3E−27	0.3902	0.0126	
14	150	2	1	1	000	2	0	2	46.1729	9419.1657	0.0044	7.768E−26	1.9E−26	0.8666	0.4203	
14	041	13	3	10	000	12	3	9	1405.1252	9419.3652	0.0098	2.216E−27	2.2E−28			
14	230	1	1	1	000	2	2	0	109.2690	9419.5333	0.0020	1.756E−26	9.4E−28	0.3471	0.0731	
14	230	4	0	4	000	4	2	3	217.0417	9419.6006	0.0003	6.201E−27	8.2E−28			
14	230	7	1	7	000	7	1	6	473.9175	9419.6006						
14	310	7	6	2	000	6	6	1	872.7904	9420.4012	0.0004	3.576E−26	3.3E−27			
14	310	7	6	1	000	6	6	0	872.7904	9420.4012						
14	121	8	2	6	000	7	0	7	403.1613	9420.7993	0.0004	9.106E−27	6.0E−28			
14	310	11	3	9	000	10	3	8	995.7931	9420.9709	0.0001	6.764E−26	7.7E−28	0.2716	0.0861	
14	230	3	0	3	000	4	1	4	156.3820	9421.9620	0.0004	3.753E−26	2.5E−27	0.2773	0.0688	
14	310	10	3	7	000	9	3	6	859.3924	9422.8795	0.0008	6.263E−26	5.7E−27			
14	230	4	3	1	000	5	3	2	374.4099	9423.0640	0.0011	8.393E−27	1.9E−27			
14	230	1	1	0	000	2	2	1	108.9260	9423.1170	0.0006	2.132E−26	3.3E−27	0.7403	0.0139	
14	310	11	2	9	000	10	2	8	964.8502	9423.3940	0.0011	7.403E−26	6.8E−28	0.3610	0.0339	
14	230	4	3	2	000	5	3	3	373.6657	9423.6922	0.0039	1.515E−26	3.5E−28	0.5724	0.0051	
14	310	3	3	1	000	2	2	0	109.2690	9424.4369	0.0005	6.894E−25	1.6E−26	0.4875	0.0049	
14	150	3	1	2	000	3	0	3	91.3300	9424.6442	0.0026	5.754E−26	1.2E−27	0.8905	0.1521	
14	310	3	3	0	000	2	2	1	108.9260	9424.8034	0.0006	6.914E−25	9.6E−27	0.4733	0.0037	
14	310	10	4	7	000	9	4	6	949.5772	9424.9906	0.0015	6.076E−26	1.5E−27	0.3499	0.0877	
14	150	2	1	2	000	1	1	1	29.8082	9425.1526	0.0005	6.834E−26	1.1E−25	0.5281	0.0152	BLD2O

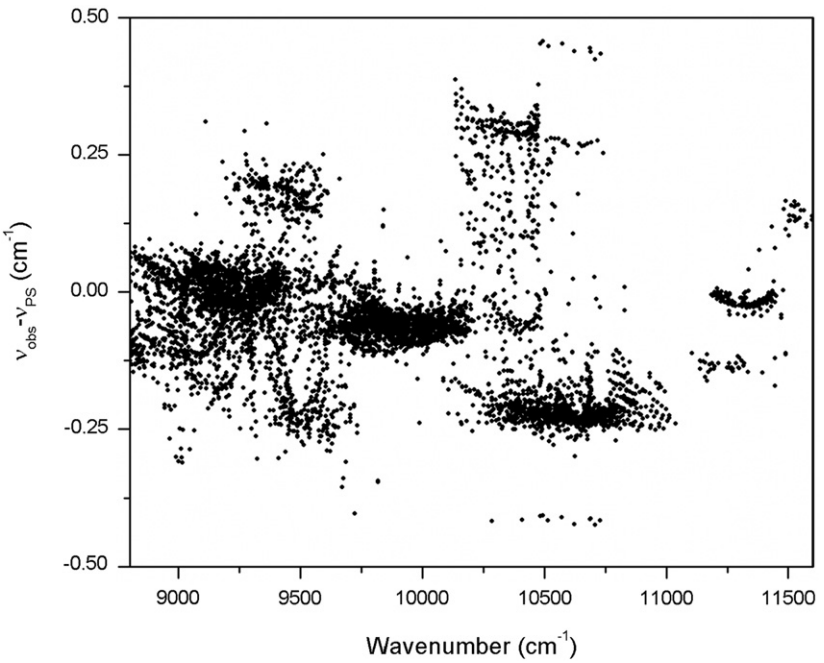

Fig. 4. ($\nu^{OBS} - \nu^{PS}$) differences between experimental and calculated $HD^{16}O$ line positions in the all 8800–11600 cm^{-1} spectral region.

in comparison with those of Ref. [21].Three of them ((041) 14 $_{3\ 12}$, (201) 13 $_{4\ 10}$ and (310) 14 $_{2\ 12}$) have been determined in [21] from one single transition for each level. According to [21] these transitions are coming from [40]: (041) 14 $_{3\ 12}$–(000) 13 $_{2\ 11}$ at 9421.410 cm^{-1}; (201) 13 $_{4\ 10}$–(000) 12 $_{2\ 11}$ at 9416.473 cm^{-1} and (310) 14 $_{2\ 12}$–(000) 13 $_{2\ 11}$ at 9433.770 cm^{-1}. We were not able to observe these lines in our recorded spectra. Corresponding energy levels were obtained from next transitions: (041) 14 $_{3\ 12}$–(000) 13 $_{3\ 11}$ at 9410.702 cm^{-1}; (201) 13 $_{4\ 10}$–(000) 14 $_{2\ 13}$ at 9033.513 cm^{-1} and (310) 14 $_{2\ 12}$–(000) 13 $_{2\ 11}$ at 9433.594 cm^{-1}. Note Ref. [40]deals with $H_2^{16}O$ lines shifts measurements and there is no $HD^{16}O$ data in this paper. The last corrected level (301) 5 $_{1\ 4}$ have been obtained in [21] from one single transition (301) 5 $_{1\ 4}$–(000) 4 $_{1\ 3}$ at 11648.661 cm^{-1} [41]. It gives the value of the (301) 5 $_{1\ 4}$ level of 11831.6445 cm^{-1}. We propose the transition (301) 5 $_{1\ 4}$–(000) 4 $_{1\ 3}$ should be assigned to the line at

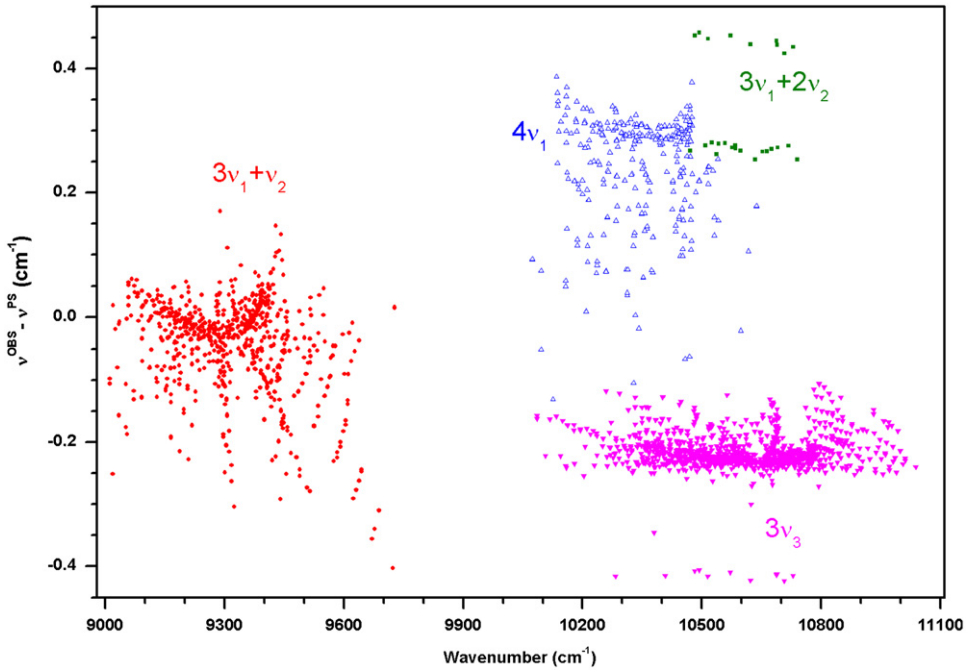

Fig. 5. ($\nu^{OBS}-\nu^{PS}$) differences between experimental and calculated $HD^{16}O$ line positions for the $3\nu_1+\nu_2$, $4\nu_1$, $3\nu_1+2\nu_2$ and $3\nu_3$ bands.

11648.5681 cm^{-1} instead of 11648.661 cm^{-1} [41]. The corresponding upper energy level is 11831.5514 cm^{-1}. It is in good agreement with our value (11831.5563 cm^{-1}, see Table 3). This value was obtained from the transition (301) 5 $_{1\ 4}$–(000) 6 $_{2\ 5}$ at 11446.681 cm^{-1}.

6. Intensities and self broadening

Line intensities are generally obtained from the two enriched spectra. The less intense lines are only measured in one spectra and some really intense lines are measured in the natural sample spectra. Great care has been taken to account for possible interference with lines of other isotopologues. In such cases the intensity of the lines of each isotopologue was determined by solving the two equations system involving the partial pressures determined as described in Section 4. Then the values of the line intensity obtained in the two spectra where compared before averaging. In case of dissagreement, some values were deleted regarding the self broadening parameter value and fitting precision consistency. As there is no absolute intensity measurements in the literature we can only compare our measurements directely to the Partidge and Schenwke calculated line list. In average, our intensities are 4% lower than the calculated ones. Table 1 gives for each vibrational band: the range of observed intensities as well as their sum. For the bands that are not too close to the limits of the spectra, this sum gives the observed band intensity.

The self-broadening values are only given when they are considered as significant (value greater than 3σ uncertainty). The high values obtained for some lines are mainly due to blended features. As for the intensities there are no experimental data in the literature. The measurements are made assuming that the broadening has no isotopic dependance. Fig. 6 shows the self-broadening value plotted as a function of the highest J and K_a values of the transitions. The plot does not give any evidence of rotational behavior so the axis is only choosen to spread the data.

7. Conclusion

In this spectral region dominated by the $HD^{16}O$ $3\nu_3$ band, the majority of the cold bands have been observed. The exceptions are the $\nu_1+6\nu_2$, $6\nu_2+\nu_3$, $\nu_1+4\nu_2+\nu_3$, $2\nu_1+2\nu_2+\nu_3$, $9\nu_2$, $4\nu_1+\nu_2$ and $\nu_1+7\nu_2$ cold bands their individual line intensity can be predicted as high as 3.4×10^{-26} cm/molec (296 K) but they are not observed due to overlapping with other $HD^{16}O$ lines or $D_2^{16}O$ and H_2^xO lines. The total integrated intensity of the observed $HD^{16}O$ lines is 1.24×10^{-20} cm/molec (292 K). The line list is given as a supplementary material to the paper. It contains for each assigned line: the HITRAN molecules and isotopologue number (14 for $HD^{16}O$), the vibration and rotation numbers of the upper and lower levels V_1 V_2 V_3 J K_a K_c, the lower state energy E_{low}, the observed line position Nu_{obs} with its uncertainty dNu both in cm^{-1}, the observed line intensity (at 292 K) I_{obs} and its uncertainty dI both in cm/molec, an estimation of the self broadening parameter γ^{self} (Gself in the ascii file) and its uncertainty $\delta\gamma$ (dG in the ascii file) both in cm^{-1}/atm at 292 K and a comment specifying that the line was blended (BL) with another species (D_2O, H_2O or $HD^{18}O$). In the case of blended lines, the individual intensities were determined, either using the area in two spectra as being the sum of the individual lines multiplied by the partial pressure ratio (when dealing with H_2O or D_2O) or using the

Table 3
New experimental energy levels of the $HD^{16}O$ molecule.

Vib	J	K_a	K_c	E^{OBS}	dE	Nt
003	9	9	1	12292.6493	1.1	1
003	9	9	0	12292.6492	1.2	1
003	10	9	2	12443.6788	1.1	2
003	10	9	1	12443.6788	1.1	2
003	10	10	1	12659.0199	1.9	1
003	10	10	0	12659.0200	1.8	1
003	11	9	3	12609.9051	1.6	1
003	12	6	6	12273.7381	.6	2
003	12	7	6	12424.2288	1.2	2
003	12	7	5	12424.2541	1.3	2
003	12	9	4	12791.2337	1.6	1
003	12	9	3	12791.2335	1.6	1
003	13	5	9	12345.9732	.8	3
003	13	5	8	12355.9935	2.0	1
003	13	6	8	12473.4202	.8	1
003	13	6	7	12474.4474	.8	2
003	13	7	7	12622.9564	1.7	1
003	13	7	6	12622.9946	1.8	1
003	14	5	10	12562.2615	1.0	1
003	14	5	9	12579.2531	1.8	2
003	15	5	10	12821.0133	2.0	1
003	16	1	15	12591.5584	1.1	2
003	16	4	13	12905.1487	1.3	1
003	17	1	16	12817.6130	1.4	1
003	17	2	16	12817.6907	1.5	1
003	17	2	15	12996.5560	2.7	1
003	17	4	14	13154.1657	2.1	1
003	18	0	18	12841.8233	2.0	1
003	18	1	18	12841.8987	1.9	1
003	19	0	19	13079.5144	2.9	1
012	8	8	1	10086.4859	.8	1
012	8	8	0	10086.4857	.9	1
012	11	7	5	10341.6241	.7	2
012	11	7	4	10341.6135	.8	2
012	11	9	3	10771.8023	1.6	1
012	11	9	2	10771.8016	1.4	1
012	12	4	8	10089.6453	.5	2
012	12	5	7	10198.9093	.6	1
012	12	6	7	10348.1352	.7	1
012	12	6	6	10348.2178	.5	2
012	12	7	6	10526.2718	.9	1
012	12	7	5	10526.2372	.8	1
012	13	3	10	10228.5519	.6	1
012	13	4	10	10266.7390	.7	2
012	13	5	9	10398.2145	.8	1
012	13	5	8	10404.7766	.5	2
012	13	6	8	10549.4115	.7	1
012	14	4	11	10481.1953	1.0	1
012	14	4	10	10533.5558	.8	2
012	14	5	10	10615.8243	1.0	1
012	14	5	9	10627.8425	1.0	1
012	14	6	8	10767.7429	1.2	1
012	15	3	13	10560.2901	1.0	1
012	15	3	12	10689.8375	1.2	1
012	15	4	12	10709.0708	.8	2
012	15	4	11	10779.8895	1.4	1
012	15	5	10	10870.0223	2.0	1
012	16	3	14	10790.0184	1.4	1
012	16	3	13	10937.2430	1.9	1
012	16	4	13	10949.8917	1.3	1
012	16	4	12	11040.6558	2.0	1
012	16	5	12	11095.0055	2.0	2
012	16	5	11	11128.7662	1.8	1
012	17	3	14	11195.3918	2.5	1
012	17	4	14	11203.2656	2.1	1
012	17	5	13	11355.7992	2.0	1
012	17	5	12	11405.0082	2.2	1

Table 3 (*continued*)

Vib	J	K_a	K_c	E^{OBS}	dE	Nt
022	9	8	2	11665.3555	1.1	1
022	9	8	1	11665.3555	1.1	1
022	9	9	1	11912.7041	1.9	1
022	9	9	0	11912.7042	1.8	1
022	10	7	4	11595.7754	1.0	2
022	10	7	3	11595.7757	1.0	2
022	10	9	2	12065.6778	2.0	1
022	10	9	1	12065.6785	3.0	1
022	11	6	6	11568.0942	.8	1
022	11	6	5	11568.1530	.7	1
022	11	7	5	11765.3306	1.0	1
022	11	7	4	11765.3307	.9	1
022	13	4	9	11678.3136	.9	2
022	13	5	9	11788.7363	1.8	1
022	13	6	8	11956.4567	1.0	1
022	14	2	12	11704.0548	.9	2
022	14	3	11	11823.1688	1.9	2
022	16	1	15	11960.4372	1.1	1
022	17	1	17	11914.9996	1.4	2
031	10	7	4	9598.6855	.6	1
032	2	2	1	11366.5650	.7	1
032	3	3	0	11503.4383	2.1	1
032	4	2	3	11473.9278	1.7	2
032	4	3	1	11565.5769	1.7	1
032	5	0	5	11460.6093	.5	1
032	5	3	2	11696.1612	.5	3
032	5	4	2	11817.4684	.7	2
032	5	4	1	11817.4699	.7	2
032	6	4	3	11911.0957	.6	1
032	6	4	2	11911.2211	.6	1
032	6	6	1	12263.0060	.7	1
032	6	6	0	12263.0059	.7	1
032	7	3	5	11897.0233	.5	1
032	7	3	4	11903.5246	.5	2
032	7	4	3	12020.9674	.5	1
032	7	5	3	12179.9999	.6	1
032	7	5	2	12180.0006	.7	1
032	8	1	7	11847.2001	2.2	1
032	8	5	4	12304.9883	2.3	1
032	8	5	3	12304.9943	2.6	1
032	9	4	5	12289.7369	.6	1
032	10	1	10	11985.5873	1.9	1
032	10	3	7	12348.3656	.6	1
041	0	0	0	9032.1027	.5	2
041	1	0	1	9047.5964	.5	2
041	2	0	2	9078.2625	.5	4
041	2	2	0	9198.7913	.6	3
041	3	0	3	9123.4314	.5	2
041	4	0	4	9182.0411	.4	3
041	4	2	3	9307.2078	.6	2
041	5	0	5	9263.9328	.4	2
041	6	0	6	9347.6026	.V5	5
041	6	1	5	9431.2237	.5	1
041	10	1	9	9965.0732	.5	1
041	10	6	5	10774.0655	.7	1
041	10	6	4	10774.0674	.8	1
041	11	5	7	10718.1655	.7	1
041	12	1	11	10300.9065	.6	1
041	13	2	12	10488.3047	.7	1
041	14	3	12	***10953.9455****	.8	1
051	1	1	1	10378.2021	.6	1
051	2	1	2	10405.3018	.6	1
051	2	1	1	10416.6860	.6	1
051	3	1	3	10445.8313	.5	1
051	3	1	2	10468.3741	.5	2
051	4	0	4	10470.9688	.6	1
051	6	1	6	10647.2331	.5	2

Table 3 (*continued*)

Vib	J	K_a	K_c	E^{OBS}	dE	Nt
051	6	2	5	10755.9193	.5	1
051	6	2	4	10773.6400	.6	1
051	7	0	7	10722.2957	.5	1
051	7	2	6	10861.1498	.5	1
051	7	2	5	10891.2734	.5	1
051	13	1	13	11539.3820	1.1	1
070	0	0	0	9086.4223	.6	1
070	1	0	1	9102.1957	.9	2
070	9	1	9	9764.1959	.6	2
070	11	0	11	10057.8589	.6	1
080	7	1	7	10740.5146	.5	1
080	8	1	7	10964.5317	.5	1
080	9	0	9	10793.3545	.5	1
080	10	1	10	11094.4678	.6	1
080	13	0	13	10355.0802	.7	1
080	13	1	13	10384.9613	.7	1
102	9	8	1	11460.9114	.9	2
102	9	9	1	11671.4514	1.1	1
102	9	9	0	11671.4513	1.2	1
102	10	8	3	11610.1790	1.0	1
102	10	8	2	11610.1791	.9	1
102	11	6	6	11425.0337	.6	3
102	11	6	5	11424.9842	.7	1
102	11	7	4	11587.9171	.9	1
102	12	5	8	11469.3678	.7	1
102	13	4	10	11548.1236	.8	1
102	13	4	9	11582.8191	..9	1
102	13	5	8	11673.2795	1.3	1
102	14	3	11	11734.1513	1.1	1
102	15	2	13	11843.7190	2.5	1
102	16	0	16	11738.4891	1.7	2
102	16	1	16	11738.5599	1.7	2
102	16	1	15	11902.7340	2.6	1
102	16	2	15	11902.7635	2.4	1
102	17	0	17	11951.9783	1.6	1
112	4	4	1	11679.9999	.6	1
112	4	4	0	11680.0524	.6	1
112	5	4	1	11756.7950	.5	1
112	5	5	1	11893.0207	.7	1
112	5	5	0	11893.0192	.7	1
112	6	3	3	11738.1465	2.3	1
112	9	1	9	11925.8081	.6	1
112	9	1	8	12039.8362	.5	1
112	10	0	10	12054.0302	.7	1
121	7	7	1	10408.8683	.8	1
121	7	7	0	10408.8681	.9	1
121	8	4	5	9966.9180	.6	2
121	9	5	4	10266.1798	.6	2
121	10	4	6	10266.6303	.4	2
121	10	5	6	10419.8621	.6	1
121	10	5	5	10420.1792	.6	1
121	11	2	9	10318.7533	.6	1
121	11	3	8	10333.7351	.6	1
121	12	3	10	10468.7781	.6	1
121	12	3	9	10532.2878	.6	1
121	14	1	14	10534.3679	1.3	1
131	1	1	0	10519.8589	.6	1
131	2	1	2	10544.0015	.6	1
131	2	2	1	10613.3352	.6	1
131	3	1	3	10585.1790	.6	1
131	3	1	2	10604.5909	.6	1
131	4	0	4	10629.7367	.6	1
131	4	2	3	10720.7578	.5	1
131	5	0	5	10698.9648	1.5	2
131	5	2	4	10796.8574	.5	1
131	5	3	3	10913.5578	.6	1

Table 3 (*continued*)

Vib	J	K_a	K_c	E^{OBS}	dE	Nt
131	5	3	2	10913.9335	1.6	1
131	6	1	5	10852.5512	.5	2
131	8	2	7	11111.2251	.5	1
131	9	1	9	11100.8358	.5	1
150	6	3	3	10079.5268	.5	2
150	6	4	3	10208.6162	.6	1
150	6	4	2	10208.6324	.6	1
150	9	1	8	10248.4708	.5	1
150	9	2	8	10282.3913	.5	1
150	10	2	8	10505.0970	.6	1
150	11	2	9	10686.3970	.6	1
150	12	1	11	10746.4570	.6	1
150	14	1	14	10889.7967	.9	1
201	10	7	4	10544.7599	.8	1
201	10	7	3	10544.7580	.7	1
201	11	6	6	10533.0717	.6	2
201	12	2	11	10211.8074	.7	2
201	12	3	9	10389.8293	.7	2
201	12	4	8	10459.7883	.6	3
201	12	7	6	10884.2777	.9	1
201	13	3	10	10594.1649	.8	1
201	13	4	10	***10637.8766****	.9	1
201	13	5	8	10764.3581	1.3	1
201	14	0	14	10411.1802	.9	1
201	14	1	14	10411.1564	1.0	1
211	2	2	0	10517.1128	.5	2
211	3	1	3	10500.9586	.6	4
211	3	1	2	10518.0021	.5	2
211	3	2	2	10561.6250	.5	3
211	3	2	1	10563.2325	.6	2
211	4	2	3	10621.3612	.6	1
211	4	3	1	10694.8038	.4	2
211	5	1	4	10662.3593	.5	1
211	5	2	4	10695.6768	.5	1
211	5	2	3	10706.9025	.5	1
211	5	3	3	10769.7449	.5	2
211	6	1	5	10757.3295	.5	1
211	6	2	4	10803.4777	.5	2
211	7	1	6	10865.8059	.5	1
211	7	2	5	10917.7171	.5	1
211	8	0	8	10891.4968	.5	2
211	8	1	8	10892.5551	.6	1
211	9	6	4	11636.5925	.6	2
211	9	6	3	11636.5627	.7	1
211	10	1	10	11135.7760	.6	1
230	8	4	4	10323.2627	.5	1
230	8	5	4	10511.6982	.6	1
230	8	5	3	10511.7049	.6	1
230	9	5	5	10647.4858	.7	1
230	9	5	4	10647.5156	.6	1
230	12	0	12	10543.8994	.7	1
230	14	0	14	10762.0985	1.0	1
301	1	0	1	11597.3128	.7	1
301	1	1	1	11610.8593	.6	1
301	1	1	0	11613.4499	.5	2
301	2	0	2	11626.1286	.6	1
301	2	1	2	11637.4738	.5	3
301	2	1	1	11645.3173	.6	2
301	3	0	3	11668.4768	.5	2
301	3	1	3	11677.2094	.6	2
301	4	0	4	11723.8087	.5	1
301	4	1	4	11729.8450	.6	1
301	4	1	3	11754.2073	.6	1
301	5	0	5	11791.2165	.5	2
301	5	1	5	11795.2267	.5	1
301	5	1	4	***11831.5563****	.5	1

Table 3 (*continued*)

Vib	J	K_a	K_c	E^{OBS}	dE	Nt
310	11	9	3	11530.3468	1.6	1
310	11	9	2	11530.3461	1.4	1
310	12	6	7	11025.0612	.7	1
310	14	2	12	***10966.3254****	.8	1V
310	16	1	16	11025.6735	1.4	1
320	1	1	1	10655.6475	.6	1
320	1	1	0	10659.0418	.6	1
320	2	2	1	10759.8157	1.4	1
400	9	4	6	11270.9190	.5	1
400	9	5	4	11400.1902	.6	1
400	9	6	4	11557.4061	.6	2
400	9	6	3	11557.4048	.7	2
400	9	7	3	11742.2749	.6	1
400	9	7	2	11742.2745	.6	1
400	10	3	7	11332.7217	.6	1
400	10	4	7	11415.8522	.7	1
400	10	6	5	11700.4119	.V6	1
400	11	1	10	11356.9373	.7	1
400	11	2	10	11360.2104	.5	2
400	11	3	9	11467.1325	.5	1
400	11	3	8	11500.8218	.6	1
400	11	4	7	11581.2865	.7	1
400	12	0	12	11388.4626	.6	2
400	12	1	12	11385.7016	1.0	1
400	12	1	11	11519.4217	.6	1
400	13	2	12	11694.0639	.7	2
400	13	3	11	11819.4548	.7	1

Notations: Vib J K_a K_c—vibration and rotation quantum numbers; E^{OBS}—experimental values of the energy levels (cm^{-1}); dE—uncertainties of the energy levels (10^{-3} cm^{-1}); Nt—number of transitions used for the energy levels determination.

* Corrected values in comparison with those of Ref. [21] (see text).

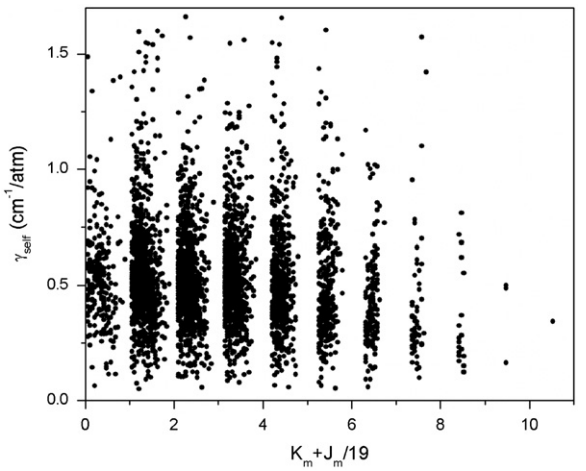

Fig. 6. Self broadening coefficients plotted as function of $(K_m+J_m/19)$ where K_m and J_m are the highest values of K_a and J, respectively, involved in the transition and 19 is the maximal value of $J+1$ for all the transitions.

calculated intensities (when dealing with $HD^{18}O$). When multiple assignment is found for one line (of the same isotopologue), the line is repeated in the list with only the line position as parameter. Finally, 289 new and four corrected energy levels belonging to 21 vibrational states of $HD^{16}O$ were obtained from the spectra analysis. The self-broadening parameters have been determined assuming that there is no isotopologue dependence and are given only when the value are significant. The data will be proposed for inclusion in the next HITRAN database as well as in the IUPAC task group [21]. The data corresponding to the $D_2^{16}O$ species will be published in a separate paper.

Acknowledgements

The French authors wish to thank the "CNRS OA-LEFE-ChAt supports" for their works on water vapor spectroscopy. This research program was also supported by the Belgian Federal Science Policy Office (contract EV/11/03C), the Fonds National de la Recherche Scientifique (FNRS, Belgium) and the European Space Agency (ESA-Prodex program).

This work was also supported by CNRS (France) and RFBR (Russia) in the frame of Groupement de Recherche International SAMIA (Spectroscopie d'Absorption des Molécules d'Intérêt Atmosphérique), as well as by RFBR-CNRS grants nos. 09-05-93105 and 10-05-93105. SM gratefully acknowledge GSMA laboratory for giving him opportunity to continue his research on absorption water spectra. Authors thank O.V. Naumenko for helpful discussions on the water spectra assignments.

Appendix A. Supplementary material

Supplementary data associated with this article can be found in the online version at doi:10.1016/j.jqsrt.2012.02.017.

References

[1] Aumann HH, Chahine MT, Gautier C, Goldberg MD, Kalnay E, McMillin LM, et al. AIRS/AMSU/HSB on the aqua mission: design, science objectives, data products, and processing systems. IEEE Trans Geosci Remote Sensing 2003;41:253–63.
[2] Bernath PF, McElroy CT, Abrams MC, Boone CD, Butler M, Camy-Peyret C, et al. Atmospheric chemistry experiment (ACE): mission overview. Geophysical Research Letters 2005;32:L15S01.
[3] Waters JW, Froidevaux L, Harwood RS, Jarnot RF, Pickett HM, Read WG, et al. The Earth Observing System Microwave Limb Sounder (EOS MLS) on the AURA satellite. IEEE Trans Geosci Remote Sensing 2006;44:1075–92.
[4] Beer R. TES on the AURA mission: scientific objectives, measurements, and analysis overview. IEEE Trans Geosci Remote Sensing 2006;44:1102–5.
[5] Clerbaux C, Hadji-Lazaro J, Turquety S, George M, Coheur P-F, Hurtmans D, et al. The IASI/MetOp1 Mission: first observations and highlights of its potential contribution to GMES2. Space Res Today 2007;168:19–24.
[6] Fischer H, Birk M, Blom C, Carli B, Carlotti M, Von Clarmann T, et al. MIPAS: an instrument for atmospheric and climate research. Atmos Chem Phys 2008;8:2151–88.
[7] Pavlenko YaV. H_2O and HDO bands in the spectra of late-type dwarfs. Astron Rep 2002;46:567–78.
[8] Jones HRA, Pavlenko Y, Viti S, Tennyson J. Spectral analysis of water vapor in cool stars. Mon Not R Astron Soc 2002;330:675–84.
[9] Béjar VJS, Zapatero Osorio MR, Rebolo R. A search for very low mass stars and brown dwarfs in the young σ Orionis cluster. Astrophys J 1999;521:671–81.

[10] Pavlenko YaV, Harris GJ, Tennyson J, HRA Jones, Brown JM, Hill C, et al. The electronic bands of CrD, CrH, MgD and MgH: application to the 'deuterium test'. Mon Not R Astron Soc 2008;386:1338–48.
[11] Olofsson AOH, Persson CM, Koning N, Bergman P, Bernath PF, Black JH, et al. A spectral line survey of Orion KL in the bands 486-492 and 541-577 GHz with the Odin satellite: I. The observational data. Astron Astrophys 2007;476:791–801.
[12] Voronin BA, Naumenko OV, Carleer M, Coheur P-F, Fally S, Jenouvrier A, et al. HDO absorption spectrum above 11500 cm^{-1}: assignment and dynamics. J Mol Spectrosc 2007;244:87–101.
[13] Mikhailenko SN, Tashkun SA, Putilova TA, Starikova EN, Daumont L, Jenouvrier A, et al. Critical evaluation of measured rotation-vibration transitions and an experimental dataset of energy levels of $HD^{18}O$. J Quant Spectrosc Radiat Transfer 2009;110:597–608.
[14] Mauguiere F, Tyuterev V, Farantos SC. Bifurcation effects and patterns in the vibrational excited states of isotopically substituted water. Chem Phys Lett 2010;494:163–9.
[15] Mérienne M-F, Jenouvrier A, Hermans C, Vandaele AC, Carleer M, Clerbaux C, et al. Water vapor line parameters in the 13000–9250 cm^{-1} region. J Quant Spectrosc Radiat Transfer 2003;82: 99–117.
[16] Tolchenov RN, Naumenko O, Zobov NF, Shirin SV, Polyansky OL, Tennyson J, et al. Water vapor line assignments in the 9250–26,000 cm^{-1} frequency range. J Mol Spectrosc 2005;233:68–76.
[17] Jenouvrier A, Daumont L, Régalia-Jarlot L, Tyuterev VG, Carleer M, Vandaele AC, et al. Fourier transform measurements of water vapor line parameters in the 4200–6600 cm^{-1} region. J Quant Spectrosc Radiat Transfer 2007;105:326–55.
[18] Bach M, Fally S, Coheur P-F, Carleer M, Jenouvrier A, Vandaele AC. Line parameters of HDO from high-resolution Fourier transform spectroscopy in the 11,500–23,000 cm^{-1} spectral region. J Mol Spectrosc 2005;232:341–50.
[19] Mikhailenko SN, Tashkun SA, Daumont L, Jenouvrier A, Carleer M, Fally S, et al. Line positions and energy levels of the ^{18}O substitutions from the HDO/D_2O spectra between 5600 and 8800 cm^{-1}. J Quant Spectrosc Radiat Transfer 2010;111:2185–96.
[20] Tennyson J, Bernath PF, Brown LR, Campargue A, Carleer MR, Csaszar AG, et al. IUPAC critical evaluation of the rotational-vibrational spectra of water vapor. Part I—energy levels and transition wavenumbers for $H_2{}^{17}O$ and $H_2{}^{18}O$. J Quant Spectrosc Radiat Transfer 2009;110:573–96.
[21] Tennyson J, Bernath PF, Brown LR, Campargue A, Csaszar AG, Daumont L, et al. IUPAC critical evaluation of the rotational-vibrational spectra of water vapor. Part II: energy levels and transition wavenumbers for $HD^{16}O$, $HD^{17}O$, and $HD^{18}O$. J Quant Spectrosc Radiat Transfer 2010;111:2160–84.
[22] Bykov AD, Lopasov VP, YuS Makushkin, Sinitsa LN, Ulenikov ON, Zuev VE. Rotation-vibration spectra of deuterated water vapor in the 9160–9390 cm^{-1} region. J Mol Spectrosc 1982;94:1–27.
[23] Bykov AD, Kapitanov VA, Naumenko OV, Petrova TM, Serdyukov VI, Sinitsa LN. The laser spectroscopy of highly excited vibrational states of $HD^{16}O$. J Mol Spectrosc 1992;153:197–207.
[24] Votava O, Fair JR, Plusquellic DF, Riedle E, Nesbitt DJ. High resolution vibrational overtone studies of HOD and H_2O with single mode, injection seeded ring optical parametric oscillators. J Chem Phys 1997;107:8854–65.
[25] Wang X-H, He S-G, Hu S-M, Zheng J-J, Zhu Q-S. Analysis of the HDO absorption spectrum between 9600 and 102,00 cm^{-1}. Chin Phys 2000;9:885–91.
[26] Hu S-M, He S-G, Zheng J-J, Wang X-H, Ding Y, Zhu Q-S. High-resolution analysis of the v_2+2v_3 band of HDO. Chin Phys 2001;10: 1021–7.
[27] Bertseva E, Naumenko O, Campargue A. The absorption spectrum of HDO around 1.0 μm by ICLAS-VECSEL. J Mol Spectrosc 2003;221: 38–46.
[28] Naumenko O, Hu S-M, He S-G, Campargue A. Rovibrational analysis of the absorption spectrum of HDO between 10,110 and 12,215 cm^{-1}. Phys Chem Chem Phys 2004;6:910–8.
[29] Ulenikov ON, Hu S-M, Bekhtereva ES, Zhu Q-S. High-resolution rovibrational spectroscopy of HDO in the region of 8900–9600 cm^{-1}. J Mol Spectrosc 2005;231:57–65.
[30] Naumenko O, Leshchishina O, Campargue A. High sensitivity absorption spectroscopy of HDO by ICLAS-VeCSEL between 9100 and 9640 cm^{-1}. J Mol Spectrosc 2006;236:58–69.
[31] Rothman LS, Gordon IE, Barbe A, Benner DC, Bernath PF, Birk M, et al. The HITRAN 2008 molecular spectroscopic database. J Quant Spectrosc Radiat Transfer 2009;110:533–72.
[32] Jenouvrier A, Mérienne MF, Carleer M, Colin R, Vandaele A-C, Bernath PF, et al. The visible and near ultraviolet rotation-vibration spectrum of HOD. J Mol Spectrosc 2001;209:165–8.
[33] Lux JP, Jenouvrier A. Réalisation d'une cellule d'absorption a réflexions multiples de grande dimension (longueur: 50 m). Rev Phys Appl 1985;20:869–75.
[34] Carleer M. Remote sensing of clouds and the atmosphere. In: Russel JE, Schafer K, Lado-Bordowski O, editors. Proceedings of SPIE, vol. 4168; 2001. p. 337–42.
[35] Vander Auwera J. Absolute intensities measurements in the v_4+v_5 band of $^{12}C_2H_2$: analysis of Herman–Wallis effects and forbidden transitions. J Mol Spectrosc 2000;201:143–50.
[36] Toth RA, Gupta VD, Brault JW. Line positions and strengths of HDO in the 2400–3300 cm^{-1} region. Appl Opt 1982;21:3337–47.
[37] Flaud JM, Camy-Peyret C, Mahmoudi A, Guelachvili G. The v_2 band of $HD^{16}O$. Int J Infrared Millimeter Waves 1986;7:1063–90.
[38] Partridge H, Schwenke DW. The determination of an accurate isotope dependent potential energy surface for water from extensive ab initio calculations and experimental data. J Chem Phys 1997;106:4618–39.
[39] Schwenke DW, Partridge H. Convergence testing of the analytic representation of an ab initio dipole moment function for water: improved fitting yields improved intensities. J Chem Phys 2000;113: 6592–7.
[40] Petrova TM, Sinitsa LN, Solodov AM. H_2O lines shifts measurements in the 1.06 μm region. Proc SPIE 2007;6936:693602.
[41] Campargue A, Vasilenko I, Naumenko O. Intracavity laser absorption spectroscopy of HDO between 11,645 and 12,330 cm^{-1}. J Mol Spectrosc 2005;234:216–27.